

Samuels-Crow Kimberly, Ellen (Orcid ID: 0000-0003-3168-9608)

Litvak Marcy (Orcid ID: 0000-0002-4255-2263)

# Atmosphere-Soil Interactions Govern Ecosystem Flux Sensitivity to Environmental Conditions in Semiarid Woody Ecosystems over Varying Timescales

Kimberly E. Samuels-Crow<sup>1</sup>, Kiona Ogle<sup>1,2,3</sup>, Marcy E. Litvak<sup>4</sup>

- (1) School of Informatics, Computing, and Cyber Systems, Northern Arizona University, Flagstaff, AZ, USA;
- (2) Department of Biological Sciences, Northern Arizona University, Flagstaff, AZ, USA;
- (3) Center of Ecosystem Science and Society, Northern Arizona University, Flagstaff, AZ, USA;
- (4) Department of Biology, University of New Mexico, Albuquerque, NM, USA

## **Key Points**

- 1. ET and NEE were more sensitive to VPD and deep soil moisture in a ponderosa pine forest than a pinyon-juniper site but otherwise responded similarly to drivers.
- 2. Net sensitivity of ET and NEE to drivers varied temporally, reflecting seasonal changes in prevailing conditions, interactions between drivers, and timing of precipitation
- 3. Antecedent deep soil moisture and precipitation were important drivers of ET and NEE, especially at the drier pinyon-juniper site

This article has been accepted for publication and undergone full peer review but has not been through the copyediting, typesetting, pagination and proofreading process which may lead to differences between this version and the Version of Record. Please cite this article as doi: 10.1029/2019JG005554

## Abstract

Water and CO<sub>2</sub> flux responses (e.g., evapotranspiration [ET] and net ecosystem exchange [NEE]) to environmental conditions can provide insights into how climate change will affect the terrestrial water and carbon budgets, especially in sensitive semiarid ecosystems. Here, we evaluated sensitivity of daily ET and NEE to current and antecedent (past) environment conditions, including atmospheric (vapor pressure deficit [VPD] and air temperature [T<sub>air</sub>]) and moisture (precipitation and soil water) drivers. We focused on two common southwestern U.S. ("Southwest") biomes: pinyon-juniper woodland (*Pinus edulis, Juniperus monosperma*) and ponderosa pine forest (*Pinus ponderosa*). Due to differences in aridity, rooting patterns, and plant physiological strategies (stomatal and hydraulic traits), we expected ET and NEE in these ecosystems to respond differently to atmospheric and moisture drivers, with longer response timescales in the drier pinyon-juniper woodland. Net sensitivity to drivers varied temporally in both ecosystems, reflecting the integrated influence of interacting drivers and antecedent precipitation patterns. NEE sensitivity to VPD and soil moisture (and ET sensitivity to deep soil moisture [S<sub>deep</sub>]) was higher in the ponderosa forest. ET and NEE in both ecosystems responded almost instantaneously to Tair, VPD, and shallow soil moisture (S<sub>shall</sub>), and increases in any of these drivers weakened the carbon sink and enhanced water loss. Conversely, S<sub>deep</sub> and precipitation influenced ET and NEE over longer timescales (days to months, respectively), and higher S<sub>deep</sub> enhanced the carbon sink. As climate changes, these results suggest hotter and drier conditions will weaken the carbon sink and exacerbate water loss from Southwest pinyon-juniper and ponderosa ecosystems.

## **Plain Language Summary**

Water and CO<sub>2</sub> move between ecosystems and the atmosphere. As climate changes, understanding what controls water loss and CO<sub>2</sub> exchange becomes more important. In dry

areas like the southwestern U.S. ("Southwest") the amount of water ecosystems lose to the atmosphere is a significant part of the water balance. CO<sub>2</sub> that moves between the atmosphere and ecosystems in dry regions is an important source of variability in carbon stored in vegetation globally. We used six years of measurements from two important ecosystems in the Southwest to understand how, and over what timescales, environmental conditions (temperature, atmospheric dryness, precipitation, and soil moisture) control the movement of water and CO<sub>2</sub> between the land and atmosphere. We focused on ponderosa pine and pinyon-juniper ecosystems because they comprise most woodlands in the Southwest. We found that both ecosystems responded to similar drivers. However, the ponderosa pine forest was more sensitive to atmospheric dryness and soil moisture. The pinyon-juniper woodland responded more to past precipitation and deep soil moisture. Sensitivity to each environmental condition varied during growing seasons with changes associated with precipitation. In general, hotter and drier conditions increased the amount of carbon and water each ecosystem lost to the atmosphere.

Acci

## Introduction

Drylands cover nearly 47% of Earth's land surface (Reynolds, 2001), support ~20% of the world's population (Reynolds & Stafford-Smith, 2002), and are expanding as climate changes (e.g., Huang et al., 2016; Mankin et al., 2017; Schlaepfer et al., 2017; Trenberth et al., 2014; Xia et al., 2016; Zhang et al., 2015). Semiarid and arid ecosystems within these regions have been identified as major modulators of CO<sub>2</sub> exchange between the land and atmosphere globally, but models remain under-constrained across these regions (Ahlström et al., 2015; Biederman, et al., 2017; Vargas et al., 2010). While the combinations of drivers most important for ET and NEE vary across dryland biomes (Law et al. 2002; Richardson et al. 2007), previous studies on CO<sub>2</sub> and H<sub>2</sub>O fluxes suggest the importance of climatic drivers (e.g., Baldocchi et al., 2018; Ellison et al., 2017; Morillas et al., 2017; Sandvig & Phillips, 2006; Y. Zhang et al., 2016). Additionally, antecedent (past) ecosystem states, disturbances, and environmental conditions can influence future ecosystem responses in drylands, often with considerable delays between the timing of a significant environmental event (e.g., drought, rain inputs, frost events) and the full ecosystem response (e.g., Anderegg et al., 2015; Ogle et al., 2015; Peltier et al., 2016; Ryan et al., 2015; Liu et al., 2019). Quantifying biome-specific sensitivity of ET and NEE to environmental drivers, and the timescales over which these drivers govern ET and NEE (Williams et al., 2009) provides important constraints on water (Bradford et al., 2006, 2014; Lauenroth & Bradford, 2006; Parton, 1978; Sala et al., 1992) and carbon (Wang & Dickinson, 2012; Zhang et al., 2017) budgets across multiple scales (e.g., local, regional, to global), especially in the context of climate change.

Here, we evaluate and compare the climatic controls on NEE and ET in two important tree-dominated semiarid biomes in the southwestern U.S. (hereafter, the "Southwest"): a ponderosa pine (*Pinus ponderosa*) forest (US-Vcp) and a pinyon-juniper woodland (US-Mpj) co-dominated by *Pinus edulis* and *Juniperus monosperma*. These two biome types are

ubiquitous across the region and have experienced increased mortality since the start of the 21<sup>st</sup> century (McDowell et al., 2016). The southwestern U.S. (hereafter, the "Southwest") is an ideal region to quantify the sensitivity of NEE and ET to combinations of drivers and their timescales of influence across arid and semiarid ecosystems. The Southwest's rugged topography juxtaposes ecosystems with different dominant vegetation over short geographic distances. Further, the Southwest generally experiences a bimodal distribution of annual precipitation, with relatively wet winters and summers (via Pacific storms and the North American Monsoon, respectively), and generally dry spring and fall (Chorover et al., 2011; Szejner et al., 2016). This precipitation pattern establishes a mechanism for lags between water inputs and fluxes (Biederman et al., 2017) and divides the growing season into distinct periods: the dry early growing season (pre-monsoon drought) and a relatively wet mid- to late-growing season that occurs after the onset of the North American Monsoon (typically July; Grantz et al., 2007).

Like many regions across the globe, climate in the Southwest has been changing, and is projected to continue changing over the next century, due to rising atmospheric CO<sub>2</sub> (e.g., Gonzalez et al., 2018; IPCC, 2013). Temperatures and drought frequency have already increased across the region (Gonzalez et al., 2018; Prein et al., 2016), triggering large-scale tree mortality events with the potential to alter the distribution and function of key ecosystems (Allen et al., 2010; Allen & Breshears, 1998; Mueller et al., 2005; Williams et al., 2012; McDowell et al., 2016, Adams et al., 2009; Anderegg et al., 2013; Breshears et al., 2013). Mean annual temperature and VPD are projected to increase across the region over the 21<sup>st</sup> century (Gonzalez et al., 2018; Jones & Gutzler, 2016; Seager et al., 2007; Seager & Ting, 2017). Although winter precipitation is expected to decrease, average annual precipitation may remain relatively unchanged (Garcia-Forner et al., 2016; Gonzalez et al., 2018; Grantz et al., 2007; Jones & Gutzler, 2016; Mankin et al., 2017; Schwalm et al., 2012;

Seager et al., 2007; Ting et al., 2018; Williams et al., 2012). Trees in many Southwest ecosystems rely on winter precipitation to recharge soil moisture (Baek et al., 2017; Kerhoulas et al., 2017), thus projected decreases in winter precipitation (Jones & Gutzler, 2016) will likely suppress ecosystem productivity and carbon sequestration (Knowles et al., 2018). It is becoming increasingly important to understand how these climate factors interact to drive ecosystem fluxes and the timescales over which these conditions are significant.

Specifically, our study is motivated by the following questions: (1) Do ET and NEE in two distinct dryland biomes respond similarly to atmospheric (e.g., VPD and Tair) and moisture-related (e.g., soil moisture or precipitation) drivers? While we expect fluxes in the pinyon-juniper woodland and ponderosa pine forest to respond similarly to the same key environmental drivers we predict that fluxes at the ponderosa pine site are more sensitive to soil moisture recharge during the monsoon and to VPD (regardless of season) due to the predominantly isohydric response of *P. ponderosa* in contrast to the more drought-tolerant behavior of J. monosperma (Anthoni et al., 1999; Dore et al., 2010; Manrique-Alba et al., 2018; Martínez-Vilalta & Garcia-Forner, 2017; McDowell et al., 2008; Voelker et al., 2018) (2) In each biome, how does the overall (or net) sensitivity of ET and NEE to each environmental driver, and interaction between environmental drivers, vary over time? In both ecosystems, we expect the net response of both fluxes to each driver to be temporally variable due to interactions with other drivers. In particular, we expect the magnitude and temporal variability in the net sensitivities of both fluxes to soil moisture and VPD to be greater at the ponderosa pine site (more sensitive) due to the different hydraulic characteristics of the dominant tree species. Finally, (3) how important are antecedent (past) environmental conditions for driving NEE and ET at each site? We expect NEE and ET fluxes at both sites to respond to antecedent drivers, but the importance of antecedent conditions is likely to be greater at the drier pinyon-juniper site (Liu et al., 2019).

We addressed our research questions by synthesizing six years of daily NEE and ET flux observations and associated climate and environmental data at each site using a Bayesian framework. The approach we employed enables quantification of time-varying environmental sensitivities and inference about the timescales over which the environmental drivers influence ET and NEE. Our results will advance our understanding of how water and carbon fluxes in these two tree-dominated biomes respond to climate drivers that are likely to change as global climate changes.

#### 2. Methods

## 2.1. Field Sites

This study uses multi-year data from two sites in the New Mexico Elevation Gradient (NMEG) (Anderson-Teixeira et al., 2011), an array of eddy covariance towers in the AmeriFlux network (Baldocchi et al., 2001; Law, 2005). The sites and instrumentation used to obtain data for this study and methods used for quality control and gap-filling across the NMEG have been described in detail elsewhere (Anderson-Teixeira et al., 2011; Morillas et al., 2017), but we provide a summary here. The flux towers span an elevation gradient of ~1200 m in central to northern New Mexico, U.S., with ecosystems that range from desert grasslands to subalpine mixed conifer forests. This study compares two sites within the NMEG network, a pinyon-juniper woodland (US-Mpj) and a ponderosa pine forest (US-Vcp). We focus on these two sites for three primary reasons. First, these two sites represent major tree-dominated ecosystems common to the Southwest that are particularly sensitive to drought and climate change (Allen et al., 2010; Allen & Breshears, 1998; Breshears et al., 2013; Huang et al., 2015; Mueller et al., 2005; Petrie et al., 2015; Shaw et al., 2005). Second, the number of co-occurring species at these sites is small, so it is likely that the dominant tree

species primarily control ecosystem fluxes. Third, relatively long (2008-2014), continuous records of ecosystem fluxes and environmental driver data are available for these sites.

The lower elevation, pinyon-juniper woodland site (US-Mpj) is located in central New Mexico just south of Mountainair, NM (elevation = 2196 m). The site is dominated by two tree species, pinyon (*P. edulis*) and one-seed juniper (*J. monosperma*), with an open canopy and an herbaceous understory comprised mainly of blue grama (*Bouteloua gracilis*), a C4 grass common to the region. The higher-elevation (2500 m) site (US-Vcp) is located approximately 150 miles northwest of US-Mpj on the flanks of a resurgent volcanic dome in the Jemez Mountains of northern New Mexico, and is dominated by *P. ponderosa* (ponderosa) with an oak (*Quercus gambelii*) understory and minimal herbaceous species cover in the footprint of the flux tower. At the US-Vcp site, average canopy height is 18-20 m within the footprint of the 25 m high tower. At the US-Mpj site, average canopy height is 2.8 m, and the flux tower is 9 m tall (Morillas et al., 2017). Both sites are relatively flat with slopes of less than 5% in the footprint of the towers. Soils at US-Mpj are Turkey Springs stony loam soils and alluvially deposited limestone that generates a shallow, discontinuous petrocalcic horizon or "caliche" layer between 30 and 80 cm depth. Soils at US-Vcp are Jaramillo loam soils that are well-drained.

Although mean annual temperature (MAT) at the US-Mpj site is only 0.7°C warmer than the US-Vcp site (10.5 °C vs 9.8 °C, respectively), US-Mpj receives 30% less precipitation (385 vs 550 mm) per year and has a lower aridity index (0.34 vs 0.53), indicative of drier average conditions (aridity index extracted from CGIAR-CSI Global-PET Dataset [http://www.cgiar-csi.org/data/global-aridity-and-pet-database], downloaded on 20 April 2017 (Zomer et al., 2007, 2008)). Both sites receive ~47% of their total annual precipitation during the North American Monsoon period (summer). Partitioned gross primary production (GPP) fluxes indicate that trees at both sites are active in spring and summer, so we focus

here on NEE and ET measured during this growing season. The growing season varies interannually with increased GPP starting between March and April at both sites and ending by October. In order to be consistent between sites, we chose to model fluxes from April to October ("growing season").

Ecosystem-atmosphere exchange of carbon and water was measured at both sites using open-path eddy covariance. Eddy covariance instrumentation was identical at both sites (LI-7500 open-path infrared gas analyzer (LI-COR, Lincoln, NE, USA), a CSAT-3 sonic anemometer (Campbell Scientific Logan, UT, USA). 10Hz data were logged with a Campbell Scientific CR5000 at both sites, and thirty-minute covariances were corrected for air density fluctuations due to temperature (Webb et al., 1980), and frequency response (Massman, 2000) using Matlab scripts (Anderson-Texiera et al. 2011; Morillas et al. 2017). Measurements from both sites were filtered for conditions that could compromise data quality, including low-turbulence conditions ( $u^* < 0.16 \text{ ms}^{-1}$ ), during precipitation pulses, non-optimal wind directions (+30° behind the tower), and instrument malfunctions (Morillas et al., 2017). We used directly measured net CO<sub>2</sub> and water fluxes (i.e., NEE and ET) for data analysis and modeling, rather than partitioned fluxes (i.e., GPP, Reco, or transpiration derived from tree-level sap-flow), to minimize additional sources of error or uncertainty associated with partitioning the measured fluxes. We did, however, partition NEE into the main components GPP and Reco by estimating respiration from night-time NEE measurements and extrapolation to daytime (Reichstein et al. 2005), and calculated GPP as (NEE + R<sub>eco</sub>), to help interpret model results (Fig. S1).

Air temperature (T<sub>air</sub>) and relative humidity ([used to calculate VPD] (HMP45C Vaisala, Helsinki, Finland), photosynthetically active radiation [PAR]( (LI-190SB, Licor Bioscience), were recorded as 30-minute averages and precipitation (TE525MM-L50 tipping bucket rain gauge, Texas Electronic) was recorded as 30-minute sums at both sites. Soil moisture

measurements were made in four to six profiles per site at depths of 0-5 cm ("shallow,"  $S_{shall}$ ) and 25-30 cm ("deep,"  $S_{deep}$ ) using Campbell Scientific CS 616 probes (Anderson-Teixeira et al., 2011). Gaps in the PAR data at US-Vcp were filled using linear interpolation; only 13% of the daily PAR observations were missing across all growing seasons. No data were missing in 2009 and 2011, and the mean gap length in the 2010, 2012, 2013, and 2014 growing season was 11 days. Figure 1 shows growing season fluxes along with continuous micrometeorological and soil moisture data from the two sites.

We used daily sums of daytime, 30-minute NEE and ET measurements in our analyses. Gaps in 30-minute flux measurements were filled using Reddyproc (<a href="https://www.bgc-jena.mpg.de/~MDIwork/eddyproc/method.php">https://www.bgc-jena.mpg.de/~MDIwork/eddyproc/method.php</a>), a freely available, web-based eddy covariance gap-filling and flux-partitioning tool based on methods described in Falge et al. (2001) and Reichstein et al. (2005). These methods primarily rely on spatial variability in radiation parameters to fill in missing flux values. At both sites, 65% to 75% of the daily, daytime ET and NEE values used in this study were based on mostly complete data (missing zero to six 30-minute daytime measurements">https://www.bgc-jena.minute daytime measurements</a>). Prior to using these methods to fill gaps in NEE and ET, any missing meteorological data were filled using data from nearby meteorological stations. The meteorological station used to gap-fill Tair and VPD at the US-Mpj site is located approximately 5 km away in a similar pinyon-juniper woodland (Morillas et al., 2017). Meteorological data used to fill in data gaps at the US-Vcp site were obtained from a weather station maintained by the Western Regional Climate Center (<a href="https://wrcc.dri.edu/weather/vjem.html">https://wrcc.dri.edu/weather/vjem.html</a>) approximately 13 km away in a similar ponderosa pine ecosystem.

#### 2.2. Data Analysis and Modeling

We implemented a stochastic antecedent model (SAM) in a Bayesian framework (Ogle et al. 2015) to evaluate the sensitivity of ET and NEE to environmental drivers, their

interactions, and the timescales over which each driver influences NEE and ET. The model specification includes a regression submodel for the flux of interest (ET or NEE) with linear, quadratic, and interactive effects of each driver (covariate). Additionally, we define a submodel to define antecedent covariates, which makes the SAM framework a non-linear regression approach. The SAM model enables evaluation of the significance of different environmental drivers and their timescales of influence. By implementing the model in a Bayesian framework, we were able to obtain full posterior distributions for quantities of interest and were able to incorporate priors that obey mass-balance-type constraints (e.g., antecedent importance weights must sum to 1; see below). The SAM approach has been successfully applied to a variety of ecological time-series data (Guo & Ogle, 2018; Ibáñez et al., 2017; Kropp et al., 2017; Ogle et al., 2015; Peltier et al., 2017), including ecosystem CO<sub>2</sub> fluxes (Barron-Gafford et al., 2014; Liu et al., 2019; Ryan et al., 2015, 2017). To explicitly evaluate the importance of antecedent environmental conditions and interactions among environmental drivers, we compared results from the "full SAM" model to simpler models that (1) considered concurrent environmental conditions only ("current only" model) or (2) removed all non-linear effects (i.e., quadratic terms and all two-way interactions; "main effects SAM" model).

For the three model variants, we assumed that the observed flux (Y = ET or NEE) measured on day i follows a normal distribution such that  $Y_i \sim Normal(\mu_i, \sigma^2)$ , where  $\mu_i$  is the mean or predicted flux and  $\sigma^2$  describes the residual variance about this mean. We modeled  $\mu_i$  as a linear regression on potentially important antecedent environmental variables (covariates; see Table 1). To capture potential non-linear responses, we included quadratic terms for atmospheric drivers, and two-way interactions among most drivers (see Table 1). For observation i and covariate j or k, the mean model is defined as:

$$\mu_{i} = \beta_{0} + \sum_{j=1}^{7} \beta_{j} X_{j,i} + \sum_{j=1}^{2} \beta_{7+j} X_{j,i}^{2} + \sum_{j=1}^{4} \sum_{k=j+1}^{5} \beta_{j,k} X_{j,i} X_{k,i}$$
 (1)

The main effects of each covariate are depicted by  $\beta_1$ ,  $\beta_2$ , ...,  $\beta_7$ , the quadratic effects of VPD and  $T_{air}$  are described by  $\beta_8$  and  $\beta_9$ , respectively, and the two-way interactions among the first five covariates are described by  $\beta_{1,2}$ ,  $\beta_{1,3}$ , ...,  $\beta_{4,5}$  (see Table 1). For covariate j and day i,  $X_{j,i}$  is based on standardized values,  $Z_{j,i}$ , of each measured covariate (see equation (2)) such that  $Z_{j,i} = (x_{j,i} - \overline{x}_j)/sd_j$ , where  $x_{j,i}$  is the original observation of covariate j on day j, and j and j are the sample mean and standard deviation computed across all observations of covariate j (equation 2, below, describes the relationship between j and j and j and j are therefore, unitless and on the same scale, facilitating direct comparison of the magnitude of the main effects. Further, j (intercept) describes the predicted flux at average environmental conditions. For the main effects SAM model, we excluded all quadratic terms and two-way interactions.

For both the full and main effects SAM models, covariates (X's) in equation (1) represent the antecedent values of the observed environmental drivers. The SAM approach specifies a stochastic model that calculates each antecedent covariate as a weighted average of past values:

$$X_{j,i} = \sum_{t=0}^{Tlag} w_{j,t} Z_{j,i-t}$$
 (2)

We interpret the antecedent importance weights  $(w_{j,t})$  as the relative importance of covariate j at varying time periods t into the past for driving the response of interest (i.e., NEE or ET). Each  $w_{j,t}$  is constrained between 0 and 1 and sums to 1 across all past time steps  $(t = 0, ..., T_{lag})$ . The magnitude of the w's, therefore, reveal timescales of influence for each individual driver or covariate (Ogle et al., 2015). For all covariates except precipitation, we used a daily time step for t, with  $T_{lag} = 6$  days; that is, t = 0 is concurrent with (same day as) the flux

measurement, t = 1 is the previous time step (i.e., yesterday), t = 2 represents two days prior, and  $t = T_{lag}$  represents conditions 6-days prior.

Precipitation ( $X_5$ ) is integrated over a 6-month period at varying time steps, ranging from weeks (t = 0, 1, 2, or 3 weeks, covering the month leading up to the flux measurement) to months (t = 4, 5, ..., 8, representing 2, 3, ..., 6 months prior). See supplemental information for details. We set  $w_{5,0} = 0$  such that precipitation received during the week leading up to the flux measurement is not considered since antecedent soil moisture over the past week is already included in the model, and NEE and ET are expected to respond directly to soil moisture at this timescale.

For the current only model, we simply set  $X_{j,t} = Z_{j,t}$ , which is equivalent to setting  $w_{j,t} = 1$  for the current time step (t = 0) and  $w_{j,t} = 0$  for all past time steps (t = 1, 2, ...). We excluded precipitation from the current model variant because we accounted for current soil moisture conditions, and current precipitation (defined as precipitation received the week leading up to the flux measurement) is not included in any of the models. Shallow soil moisture measurements integrate moisture from the surface to 5-cm depth, which should capture the moisture source involved in rapid ET responses to small precipitation events. Similarly, concurrent precipitation is not used in the SAM model variants.

We completed the model specification by assigning priors to all unknown, stochastic parameters. We chose relatively non-informative conjugate priors for the regression coefficients such that each  $\beta$  term was assigned a  $Normal(0,10^5)$  prior, where  $10^5$  is the prior variance. We specified a wide, uniform prior for the standard deviation describing the distribution of  $Y_i$  such that  $\sigma \sim Uniform(0,1000)$ . Finally, we specified a relatively non-informative Dirichlet prior for each vector of antecedent weights,  $\mathbf{w}_j = (w_{j,0}, w_{j,1}, ..., w_{j,Tlag})$ , such that  $\mathbf{w}_i \sim Dirichlet(\mathbf{1})$ , where  $\mathbf{1}$  is a vector of 1's of length  $T_{lag}+1$ . The model was fit

separately to the NEE and ET data for each site, producing four sets of parameter estimates (2 flux variables  $\times$  2 sites) for each of the three model variants.

## 2.3. Evaluating the Net Effect of Each Driver

We evaluated the net sensitivity of each flux variable to each antecedent driving variable (covariate) by computing the partial derivative of  $\mu$  (equation (1)) with respect to the covariate of interest, X. For example, the net sensitivity of predicted NEE or ET to antecedent  $T_{air}(X_1)$  is given by:

$$\frac{\partial \mu_i}{\partial X_1} = \beta_1 + 2\beta_8 X_{1,i}^2 + \sum_{k=2}^5 \beta_{1,k} X_{k,i}$$
 (3)

Computation of  $\partial \mu/\partial X$ , as illustrated by  $\partial \mu/\partial X_1$ , accounts for uncertainty in the antecedent weights and regression coefficients, producing posterior distributions for the sensitivity indices. In general, when  $\partial ET/\partial X$  is positive, ET increases (decreases) in response to an increase (decrease) in the driver, X. When  $\partial NEE/\partial X$  is positive, an increase in the driver leads to less negative (or more positive) NEE, indicating an increased contribution of  $R_{eco}$  relative to GPP (e.g., increased carbon loss to the atmosphere), while a decrease in the driver leads to more negative (or less positive) NEE (relatively high GPP component or carbon gain). In contrast, when  $\partial NEE/\partial X$  is negative, a decrease (increase) in the driver leads to increasingly positive (increasingly negative) NEE.

## 2.4. Model Implementation and Fit

We coded the models in JAGS 4.0.0 (Plummer, 2003) and implemented each through R (Core Team, 2015), using the rjags package. For each model variant (i.e., current only, main effects SAM, and full SAM), we sampled the posterior parameter space and assessed convergence using three parallel MCMC chains run for 40,000 iterations. We subsequently thinned the chains to produce  $\geq$  3,000 approximately independent posterior samples for each

quantity of interest. We assessed convergence using the Gelman and Rubin (1992) diagnostic. Parameter estimates are reported as the posterior means and 95% credible intervals (CIs), defined by the 2.5<sup>th</sup> and 97.5<sup>th</sup> percentiles.

We evaluated model fit for each model variant by computing the coefficient of determination ( $R^2$ ) from a regression of the observed fluxes (Y = NEE or ET) on the predicted fluxes given the fitted values for  $\mu_i$  and  $\sigma$  (i.e., using replicated data, as per Gelman et al. 2013). We compared  $R^2$  values among models, in addition to coverage (i.e., percent of observations contained within the 95% CIs of the corresponding replicated data). Increasingly complex models are accompanied by improved model fit, so we accounted for this artifact of model complexity by calculating the Deviance Information Criterion (DIC) for each model variant (Spiegelhalter et al., 2002). DIC, although imperfect (Gelman et al., 2013; Spiegelhalter et al., 2014), corrects model fit for model complexity by taking into account the effective number of parameters in the model (pD). When DIC calculated for models of different complexity differs by 10 or more, the model with the lower DIC is preferred (Spiegelhalter et al., 2002).

## 2.5 Evaluating Model Sensitivity to Data Selection

We conducted tests to evaluate model sensitivity to (1) start of the growing season and (2) percent of gap-filled 30-minute data. Model sensitivity tests indicate that the April to October growing season captured the period significant for biological activity at both sites. Changing the defined growing season to March for the US-Mpj site, which is warmer and becomes active earlier in the year, did not significantly change the results (Table S1 and S4). Excluding gap-filled data did not significantly change our results (see Supplemental Materials, section B).

## 3. Results

#### 3.1. Model Fit

All three model variants reproduced measured fluxes reasonably well. For the full SAM model, regressions of observed versus predicted observations produced R<sup>2</sup> values of 0.65 and 0.68 for NEE at US-Vcp and US-Mpj, respectively, and 0.72 and 0.77 for ET at US-Mpj and US-Vcp, respectively (Fig. 2 and Fig. S2). Nominal coverage probabilities (i.e., the percent of measured values that fall within the 95% Bayesian credible interval (CI) of their corresponding replicated data values) indicate that the full SAM model replicates the temporal variation in growing season fluxes well. At both sites, 95% to 96% of the measured ET and NEE values fall within this 95% (CI) of their corresponding replicated data values (Fig. S3). Including only current covariates or only main effects (i.e., current only or main effects SAM model variants) led to R<sup>2</sup> values that were approximately 6% lower for ET at both sites and 9% to 13% lower for NEE at US-Mpj and US-Vcp, respectively (Fig. 2). Further, DIC for the full SAM variant was consistently lower by at least 24 units (Table S2), indicating that the full SAM variant provided the best model fit and that main effects or current conditions alone were inadequate to explain the variability in NEE and ET at each site.

Since the full SAM variant provided the best model fit, we evaluated the posterior results of this model variant to compare the sensitivity of ET and NEE to atmospheric and moisture-related covariates across the two ecosystems. The full SAM variant further allowed a comparison of the timescales over which each covariate exerts the greatest influence on ET and NEE. Finally, the full SAM model allowed an analysis of temporal variations in the net sensitivity of each flux to environmental drivers,  $\partial \mu / \partial X$ , across each growing season that emerge from interactions between covariates.

## 3.2. Significant Drivers of ET and NEE

NEE and ET at both sites respond similarly to the main atmospheric and moisture-related drivers (Table 1). Increases in  $T_{air}$  and  $S_{shall}$  generally enhanced water and  $CO_2$  loss at both sites. Increased VPD also enhanced  $CO_2$  loss while dampening water loss at both sites. In contrast, increased PAR and/or  $S_{deep}$  enhanced  $CO_2$  storage in both ecosystems while increasing ET (Table 1; Table S1a and S1b). The range of VPD ( $\Delta$ VPD) in a given day exerted an influence over both fluxes at US-Vcp but not at US-Mpj.

Although the main and quadratic effects contribute to the net effect of each driver on each flux, they do not tell the whole story. For example, the main effects of precipitation were insignificant for driving CO<sub>2</sub> fluxes at both sites, but there were significant interactions between precipitation and other drivers (Table 1; Table S1a and S1b). In addition, higher VPD dampens ET at both sites, but there are significant interactions between VPD and other climate drivers (Table 1) that make this result difficult to interpret without calculating net sensitivity, which simultaneously considers the main, quadratic, and interaction effects along with antecedent influences (see Section 3.3).

## 3.3. Temporal Variability in Net Sensitivity to Drivers

The net sensitivity of ET and NEE to each driver (i.e.,  $\partial \mu/\partial X$  [equation 3]) is generally consistent with parameter estimates for the main effects (Table 1) but varies temporally due to interactions with other covariates and is often stronger than the p-values of sensitivity to main drivers would suggest. The net sensitivity of ET and NEE varied both within growing seasons and across years (e.g., Fig. 3 and 4). Here, we focus on the net sensitivity of ET and NEE to the key atmospheric ( $T_{air}$  and VPD) and soil moisture ( $S_{shall}$  and  $S_{deep}$ ) drivers that govern these fluxes.

Consistent with the main effects,  $\partial ET/\partial T_{air}$  (Fig. 3a) and  $\partial ET/\partial S_{shall}$  (Fig. 3c) were positive across the growing season in all years at both sites, indicating that ET increased in response to increases in these drivers (i.e.,  $T_{air}$  and  $S_{shall}$ ). Differences between the two sites,

however, emerge in the intraseasonal variability in the net sensitivity to  $T_{air}$ ; At US-Mpj,  $\partial ET/\partial T_{air}$  increased in the middle of the growing season, whereas  $\partial ET/\partial T_{air}$  gradually decreased over the growing season at US-Vcp, often with a steep decline in July. These changes at both sites generally accompanied increased precipitation in the middle of the growing season (Fig. 3e), associated with the onset of the North American Monsoon. The temporal variation in  $\partial ET/\partial S_{shall}$  was nearly identical at both sites, and was generally highest early in the growing season (Fig. 3c).

The net sensitivities of ET to VPD and  $S_{deep}$ ,  $\partial ET/\partial VPD$  (Fig. 3b) and  $\partial ET/\partial S_{deep}$  (Fig. 3d), respectively, were also generally consistent with the main effects of those drivers. For the most part,  $\partial ET/\partial VPD$  was negative throughout the growing season at both sites, meaning that ET decreased in response to increased VPD (Fig. 3b). While this is consistent with the main effect of VPD on ET ( $\beta_2$ , Table 1),  $\partial ET/\partial VPD$  increased around the middle of the growing season at the US-Vcp site in most years. There was less consistent intraseasonal variability at US-Mpj. Like the ET response to  $S_{shall}$ ,  $\partial ET/\partial S_{deep}$  was positive across most of the growing season. Unlike  $\partial ET/\partial S_{shall}$ , however, the magnitude and temporal variability in  $\partial ET/\partial S_{deep}$  is less consistent among the sites. The inter- and intraseasonal variability in the magnitude of  $\partial ET/\partial S_{deep}$  (Fig. 3d) is likely due to variability in the sign and magnitude of the significant interactions involving  $S_{deep}$  (Table 1) and the associated temporal variability in  $S_{deep}$  especially at the US-Vcp site (Fig. 1f). Throughout the growing season,  $\partial ET/\partial S_{deep}$  was lower at US-Mpj than at US-Vcp. At US-Vcp,  $\partial ET/\partial S_{deep}$  varied bimodally and was highest during the dry, early part of the growing season and again later in the growing season.

The magnitude of intraseasonal variability in the net sensitivity of NEE to atmospheric drivers was also similar across sites. At both sites, NEE was fairly insensitive to changes in  $T_{air}$  at the shoulder seasons ( $\partial NEE/\partial T_{air}$  close to zero) when NEE is neutral or slightly

negative (Fig. 1b). Occasional excursions of ∂NEE/∂Tair toward negative values at the beginning of the growing season at US-Vcp indicate that NEE became more negative as Tair increased, indicating increased carbon sink strength. ∂NEE/∂Tair shifted to high and significantly positive values as the growing season progressed, peaking mid-growing season (Fig. 4a). Across all growing seasons, ∂NEE/∂VPD at US-Mpj was negative (i.e., as VPD increased, NEE became more negative or less positive) or near zero (i.e., VPD did not exert a significant influence over NEE). At US-Vcp, ∂NEE/∂VPD was generally positive (i.e., NEE became more positive with increasing VPD) throughout the growing season (Fig. 4b), consistent with the main effect. Although the main effects and net sensitivities of each driver had the same sign at US-Vcp, the main effect alone did not capture the decrease in NEE sensitivity to VPD once precipitation increased in the middle of each growing season (Fig. 4b). In general, NEE at US-Vcp was more sensitive to VPD (i.e., higher magnitude for ∂NEE/∂VPD) than NEE across the growing season at US-Mpj.

The net sensitivity of NEE to moisture-related variables (e.g.,  $S_{shall}$  and  $S_{deep}$ ) was consistent with the main effects at both sites, but the main effects do not capture the temporal patterns in sensitivity, which are notably more variable at US-Vcp than at US-Mpj for both  $\partial NEE/\partial S_{shall}$  and  $\partial NEE/\partial S_{deep}$  (Fig. 4c and 4d, respectively). At US-Mpj,  $\partial NEE/\partial S_{shall}$  was positive throughout the growing season, and fairly tightly constrained (narrow 95% CIs) to relatively small values. In contrast, at US-Vcp,  $\partial NEE/\partial S_{shall}$  was often positive at the start of the growing season, dropping to negative values over a period of 1-2 months, then increasing and reaching positive values after precipitation onset (Fig. 4c and 4e). The net sensitivity of NEE to  $S_{deep}$  ( $\partial NEE/\partial S_{deep}$ ) was generally negative at both sites, but of larger magnitude at US-Vcp (Fig. 4d).

#### 3.4. Importance of Antecedent Drivers

The timescales over which individual atmospheric and moisture-related drivers influenced ET and NEE differed. At both sites, VPD,  $T_{air}$ , and  $S_{shall}$  exerted their greatest influence (i.e., highest importance weight,  $w_{j,l}$ , equation (2)) over ET (Figs. 5a and 5c) and NEE (Figs. 5b and 5d) on the day of measurement, and the influence of these variables was negligible two or more days prior to the flux measurement (Fig. 5). At US-Vcp, concurrent VPD and  $S_{shall}$  accounted for approximately 45% (posterior mean for importance weight,  $w_{j,1}$  = 0.45) of the total influence of these drivers over NEE, while concurrent  $T_{air}$  accounted for approximately 60% of the temperature influence on NEE (Fig. 3b). At US-Mpj, concurrent VPD,  $T_{air}$ , and  $S_{shall}$  exerted a stronger influence over NEE (posterior means for  $w_{j,1}$  = 0.70, 0.80, and 0.90, respectively) than ET ( $w_{j,1}$  = 0.70, 0.60, and 0.80, respectively) (Fig. 5c and d).

While  $T_{air}$ , VPD, and  $S_{shall}$  exerted an almost instantaneous influence over ET and NEE, antecedent  $S_{deep}$  and precipitation were important for driving fluxes at both sites. At US-Vcp,  $S_{deep}$  became increasingly important further into the past, with the highest importance weights occurring 6 days prior to the ET and NEE measurements (Figs. 5a and 5b). The timescales of influence of  $S_{deep}$  over ET at US-Mpj are not well resolved, whereby the importance weights did not notably vary among past time steps ( $w_{j,t} \approx 0.14$  for all t = 1, 2, ..., 7) (Fig. 3c). NEE at US-Mpj was influenced more by  $S_{deep}$  experienced a week ago (6 to 7 days in the past) than by concurrent  $S_{deep}$  (Fig. 5d).

The timescales of influence of precipitation at US-Vcp were more variable for NEE than for ET, with the highest importance weights for precipitation occurring three months prior to the NEE measurement (Fig. 5b). ET at the US-Vcp site responded more rapidly to precipitation, with the highest importance weights occurring the week prior to the flux measurement (Fig. 5a). In contrast, at US-Mpj, importance weights were highest for precipitation received four to five months prior, for both ET and NEE (Fig. 5c).

#### 4. Discussion

The goal of this study was to (1) compare ET and NEE responses to atmospheric and moisture-related drivers across semiarid ecosystems, (2) determine how the net sensitivity of these fluxes to individual climate variables vary temporally, and (3) determine the timescales over which drivers influence the fluxes.

## 4.1. ET and NEE Responses to Atmospheric and Moisture-Related Drivers

NEE and ET fluxes in both the pinyon-juniper woodland and ponderosa pine forest responded strongly to both atmospheric drivers and soil moisture status, consistent with previous studies in semiarid ecosystems (e.g., Jia et al., 2016; Jung et al., 2011, Anderson-Teixeira et al. 2011). Warmer air temperatures ( $T_{air}$ ), higher vapor pressure deficits (VPD), and greater shallow soil moisture ( $S_{shall}$ ) all decreased net carbon uptake (resulting in more positive NEE) in both sites with variable impacts on water loss (ET). In contrast, increases in deep soil moisture ( $S_{deep}$ ) in both sites increased net carbon uptake (resulting in more negative NEE).

We hypothesized that fluxes at the ponderosa pine site would be more sensitive to VPD and soil moisture because of the dominance of trees with generally isohydric properties. With the exception of the response of NEE to T<sub>air</sub> at the ponderosa pine site, the sign of the responses to these individual drivers was the same in both ecosystem types (Table 1). However, the magnitude of the response of both ET and NEE to VPD and the magnitude of the NEE response to S<sub>deep</sub> were higher at the ponderosa pine site than the pinyon-juniper woodland (Table S1a), suggesting that this hypothesis is, at least partially, supported. However, interpreting the main, or even non-linear (quadratic), effects of individual drivers can be misleading due to the presence of significant interactions between drivers (Neter, 1996). This motivated us to focus on the net sensitivities, which simultaneously account for

the interactive, main, and quadratic effects, in addition to the timescales over which each driver influences NEE and ET.

## 4.2. Temporal Variability in Net Sensitivity Across Ecosystems

The net sensitivities of NEE and ET to different drivers varied within and across seasons at both sites. We expected the net sensitivities of ET and NEE to drivers such as VPD and soil moisture to be of higher magnitude (more sensitive) and to exhibit greater temporal variability at the ponderosa pine forest compared to the pinyon-juniper woodland, again, due to the different hydraulic properties of the dominant vegetation across the sites.

In support of our hypothesis, NEE was more sensitive to VPD and soil-moisture-related drivers in the ponderosa pine forest compared to the pinyon-juniper woodland (Fig. 4b-d). At the ponderosa pine site, increased VPD reduced net CO<sub>2</sub> uptake early in the growing season. In contrast, at the start of the growing season, NEE at the pinyon-juniper site was insensitive to VPD. Overall, these results suggest that high VPD (increased atmospheric water deficit) weakens the carbon sink to a greater degree in ponderosa pine forests than in pinyon-juniper woodlands, consistent with previous studies on the effects of rising temperature across the study region (Anderson-Teixeira et al., 2011).

NEE in the ponderosa pine forest was also more sensitive, and exhibited greater intraseasonal variability, to soil moisture compared to NEE in the the pinyon-juniper woodland. Although the net sensitivity of NEE to shallow soil moisture  $(S_{shall})$ ,  $\partial NEE/\partial S_{shall}$ , was consistently positive in the pinyon-juniper woodland, there were periods when  $\partial NEE/\partial S_{shall}$  was negative at the ponderosa pine site, particularly during the pre-monsoon dry period when  $S_{shall}$  is low (Fig. 1). Unlike the response of NEE to  $S_{shall}$ , the net sensitivity of NEE to deep soil moisture  $(S_{deep})$  was generally negative throughout the growing season at both sites (Fig. 4d). This is consistent with observations that tree species at both sites rely on deep soil moisture for growth, which would lead to negative NEE, particularly early in the

growing season (Chesus & Ocheltree, 2018; Grossiord, Sevanto, Borrego, et al., 2017; Guo et al., 2018; Kerhoulas et al., 2013, 2017; West et al., 2007). Microbes within a few centimeters of the surface become active quickly when wet, so heterotrophic respiration is typically uncoupled from deeper moisture (Belnap et al., 2005). This negative sensitivity may, therefore, describe the influence of deep moisture, which is generally higher and more variable at the ponderosa pine site (Fig. 1), on photosynthesis versus heterotrophic activity.

The temporal variability in the net sensitivity of ET to atmospheric drivers and deep soil moisture also varied across sites. Again, the magnitude and temporal variability of the net sensitivity of ET to these drivers was greater at the ponderosa pine site. This was particularly true for the response to deep soil moisture. At the ponderosa pine site, ET was most sensitive to S<sub>deep</sub> early in the growing season (dry pre-monsoon) when these trees are expected to rely on deeper moisture recharged by snowmelt (e.g., Kerhoulas et al., 2013, 2017). At the pinyon-juniper site,  $\partial ET/\partial S_{deep}$  was less variable than at the ponderosa pine site, and there were periods when water loss at this site was insensitive to S<sub>deep</sub>. The lower sensitivity of ET to S<sub>deep</sub> in the pinyon-juniper woodland may reflect the relatively low and invariable moisture status of the deeper layers at this site (Fig. 1). Alternatively, it could reflect a seasonal shift to greater reliance of the trees on shallower moisture sources, as has been documented for pinyons and junipers across the region (e.g., West et al., 2007; Grossiord et al., 2017). Finally, the lower sensitivity of ET to S<sub>deep</sub> at the pinyon-juniper woodland may also be due to a more dominant role of near-surface evaporation (relative to transpiration) at this site. This near-surface soil-water evaporation is typically decoupled from the water status of the deeper soil layers, and is a dominant process even after the onset of the monsoon at similar elevations across the region (Vivoni et al., 2008).

## 4.3. Past Moisture Conditions Control CO2 and Water Fluxes

The degree to which antecedent conditions controlled carbon and water fluxes varied across the ecosystems. We hypothesized that the net carbon and water fluxes would be more sensitive to past conditions at the drier pinyon-juniper site, consistent with global studies (Besnard et al., 2019; Liu et al., 2019). This hypothesis is partially supported. In contrast to our hypothesis, however, fluxes in both ecosystems responded similarly and almost instantaneously to atmospheric drivers and shallow soil moisture (Fig. 5). In support of our hypothesis, while both antecedent precipitation and deep soil moisture were important at both sites, we observed longer response timescales for these driving variables at the pinyon-juniper woodland. In the ponderosa pine forest, precipitation received one week to three months prior to the flux measurement exerted the most significant influence over ET and NEE, respectively. In contrast, precipitation received 5-6 months prior influenced both NEE and ET in the pinyon-juniper woodland.

Globally, the timescales over which soil moisture and precipitation influence NEE are highly variable in forested ecosystems (1.5 to 7.5 months), with longer timescales reported for drier ecosystems (Liu et al., 2019). Our results for both ET and NEE are consistent with this finding, though the mechanisms that give rise to these long timescales are poorly understood. One possibility is that the 3 to 6 month timescale reflects the importance of winter precipitation to NEE and ET, similar to observations at other sites (Baek et al., 2017; Guo et al., 2018; Kerhoulas et al., 2017), For example, winter precipitation, especially snow, is important for moisture recharge of deeper soil depths (> 30 cm) and the subsequent stimulation of root development (Loik et al., 2013). The longer response timescales of fluxes to precipitation inputs at the pinyon-juniper site, compared to the ponderosa pine site, is consistent with precipitation exerting longer timescales of influence over NEE under more arid conditions (Liu et al., 2019). Moreover, the comparatively long timescales over which precipitation influences NEE and ET, and the multiple significant interactions between the

short timescale drivers and precipitation (Table 1), suggests that the precipitation regime several months prior to the flux measurement is an important determinant of the sensitivity of NEE and ET to other atmospheric- and moisture-related drivers.

#### 5. Conclusions

The significant climatic drivers of ET and NEE and the timescales over which they influence these fluxes, were similar in two semiarid coniferous biomes. Many of the drivers interacted with each other to influence ET and NEE, leading to temporal variation in the sensitivity of these fluxes to key atmospheric and moisture-related drivers. Further, we found that ET and NEE in both ecosystems responded nearly instantaneously to air temperature, vapor pressure deficit, and shallow soil moisture, but responded to deep soil moisture and precipitation over longer timescales. The mechanisms underlying these delayed and / or persistent responses are unclear, but could reflect the role of rooting depth patterns, stimulation and production of deep roots, deep soil moisture recharge dynamics, and/or delays associated with hormonal signaling, among others.

The notably long timescales over which past precipitation and deep soil moisture influence ET and NEE in both ecosystems, and the temporal variation in the flux sensitivities to climate drivers, highlights the importance of considering such temporal features when modeling ecosystem responses (i.e., NEE and ET) to environmental conditions. In the two coniferous semiarid systems studied here, temporal variation in the net sensitivities of NEE and ET are partly driven by cumulative precipitation patterns and align with the onset of the North American Monsoon. In a changing climate, factors that decrease an ecosystem's capacity to store carbon or that enhance water loss are of particular concern. In both ecosystems studied here, warmer conditions consistently led to increased CO<sub>2</sub> and water loss, while increases in deep soil moisture enhanced CO<sub>2</sub> storage. As temperatures and VPD continue to rise across the region and winter precipitation potentially decreases (Jones &

Gutzler, 2016), this combination of changes may weaken the carbon sink and exacerbate evaporative water loss across the Southwest.

## Acknowledgments

Acce

This manuscript is based on data collected at the NMEG, which continues to be supported by the DOE-Ameriflux Management Project (Subcontract No. 7074628) and the NSF-Jemez-Catalina Critical Zone Observatory (EAR1331408). The statistical analysis and modeling aspects of this study were partly supported by an NSF Advances in Biological Informatics award to K.O. (DBI#1458867). Partial support also came from an NSF Hydrologic Sciences award to K.S-C., K.O., and M.L. (EAR#1834699). Data from US-Mpj and US-Vcp can be downloaded from the AmeriFlux database (<a href="https://ameriflux.lbl.gov/">https://ameriflux.lbl.gov/</a>). Aridity and PET data are available at <a href="http://www.cgiar-csi.org/data/global-aridity-and-pet-database">https://www.cgiar-csi.org/data/global-aridity-and-pet-database</a>. Model code used in this study is available in the supplemental information. We thank Steven Crisp, Jonathan Furst, Skyler Hackley, for field assistance and data quality control, and Tomer Duman, Alex Moody, Greg Maurer and Tim Hilton for data processing. This manuscript benefited greatly from the contributions of two anonymous reviewers.

# References

- Adams, H. D., Guardiola-Claramonte, M., Barron-Gafford, G. A., Villegas, J. C., Breshears, D. D., Zou, C. B., ... Huxman, T. E. (2009). Temperature sensitivity of drought-induced tree mortality portends increased regional die-off under global-change-type drought.

  \*Proceedings of the National Academy of Sciences of the United States of America, 106(17), 7063–7066. https://doi.org/10.1073/pnas.0901438106
- Ahlström, A., Raupach, M. R., Schurgers, G., Smith, B., Arneth, A., Jung, M., ... Zeng, N. (2015). The dominant role of semi-arid ecosystems in the trend and variability of the land CO2 sink. *Science*, 348(6237), 895–899. https://doi.org/10.1002/2015JA021022
- Allen, C. D., & Breshears, D. D. (1998). Drought-induced shift of a forest-woodland ecotone. *Proceedings of the National Academy of Sciences*, 95(December), 14839–14842.
- Allen, C. D., Macalady, A. K., Chenchouni, H., Bachelet, D., McDowell, N., Vennetier, M., ... Cobb, N. (2010). A global overview of drought and heat-induced tree mortality reveals emerging climate change risks for forests. *Forest Ecology and Management*, 259(4), 660–684. https://doi.org/10.1016/j.foreco.2009.09.001
- Anderegg, W. R. L., Plavcová, L., Anderegg, L. D. L., Hacke, U. G., Berry, J. A., & Field, C. B. (2013). Drought's legacy: Multiyear hydraulic deterioration underlies widespread aspen forest die-off and portends increased future risk. *Global Change Biology*, *19*(4), 1188–1196. https://doi.org/10.1111/gcb.12100
- Anderegg, W. R. L., Schwalm, C., Biondi, F., Camarero, J. J., Koch, G., Litvak, M., ... Pacala, S. (2015). Pervasive drought legacies in forest ecosystems and their implications for carbon cycle models. *Science*, *349*(6247), 528–532. https://doi.org/10.1126/science.aab1833
- Anderson-Teixeira, K. J., Delong, J. P., Fox, A. M., Brese, D. A., & Litvak, M. E. (2011). Differential responses of production and respiration to temperature and moisture drive the carbon balance across a climatic gradient in New Mexico. *Global Change Biology*, 17(1), 410–424. https://doi.org/10.1111/j.1365-2486.2010.02269.x
- Anthoni, P. M., Law, B. E., & Unsworth, M. H. (1999). Carbon and water vapor exchange of an open-canopied ponderosa pine ecosystem. *Agricultural and Forest Meteorology*, 95(3), 151–168. https://doi.org/10.1016/S0168-1923(99)00029-5
- Baek, S. H., Smerdon, J. E., Coats, S., Williams, A. P., Cook, B. I., Cook, E. R., & Seager, R. (2017). Precipitation, Temperature, and Teleconnection Signals across the Combined North American, Monsoon Asia, and Old World Drought Atlases. *Journal of Climate*, 30(18), 7141–7155. https://doi.org/10.1175/JCLI-D-16-0766.1
- Baldocchi, D., Chu, H., & Reichstein, M. (2018). Inter-annual variability of net and gross ecosystem carbon fluxes: A review. *Agricultural and Forest Meteorology*, 249(May 2017), 520–533. https://doi.org/10.1016/j.agrformet.2017.05.015
- Baldocchi, D., Falge, E., Gu, L., Olson, R., Hollinger, D., Running, S., ... Wofsy, S. (2001). FLUXNET: A New Tool to Study the Temporal and Spatial Variability of Ecosystem-Scale Carbon Dioxide, Water Vapor, and Energy Flux Densities. *Bulletin of the American Meteorological Society*, 82(11), 2415–2434. https://doi.org/10.1175/1520-0477(2001)082<2415:FANTTS>2.3.CO;2
- Barron-Gafford, G. A., Cable, J. M., Bentley, L. P., Scott, R. L., Huxman, T. E., Jenerette, G. D., & Ogle, K. (2014). Quantifying the timescales over which exogenous and endogenous conditions affect soil respiration. *New Phytologist*, *202*, 442–454. https://doi.org/10.1111/nph.12675
- Belnap, J., Welter, J. R., Grimm, N. B., Barger, N., & Ludwig, J. A. (2005). Linkages Between Microbial and Hydrologic Processes in Arid and Semiarid Watersheds. *Ecology*, 86(2), 298–307.

- Besnard, S., Carvalhais, N., Altaf Arain, M., Black, A., Brede, B., Buchmann, N., ... Reichstein, M. (2019). Memory effects of climate and vegetation affecting net ecosystem CO2 fluxes in global forests. *PLoS ONE*, *14*(2), 1–22. https://doi.org/10.1371/journal.pone.0211510
- Biederman, J. A., Scott, R. L., Bell, T. W., Bowling, D. R., Dore, S., Garatuza-Payan, J., ... Goulden, M. L. (2017). CO2 exchange and evapotranspiration across dryland ecosystems of southwestern North America. *Global Change Biology*, (September 2016), 1–18. https://doi.org/10.1111/gcb.13686
- Bradford, J. B., Schlaepfer, D. R., Lauenroth, W. K., & Burke, I. C. (2014). Shifts in plant functional types have time-dependent and regionally variable impacts on dryland ecosystem water balance. *Journal of Ecology*, *102*(6), 1408–1418. https://doi.org/10.1111/1365-2745.12289
- Bradford, J. B., Lauenroth, W. K., John, B., & William, K. (2006). Controls over invasion of Bromus tectorum: The importance of climate, soil, disturbance and seed availability Controls over invasion of Bromus tectorum: The importance of climate, soil, disturbance and seed availability. *Journal of Vegetarion Science*, *17*(6), 693–704. https://doi.org/10.1658/1100-9233(2006)17
- Breshears, D. D., Adams, H. D., Eamus, D., McDowell, N. G., Law, D. J., Will, R. E., ... Zou, C. B. (2013). The critical amplifying role of increasing atmospheric moisture demand on tree mortality and associated regional die-off. *Frontiers in Plant Science*, 4(August), 266. https://doi.org/10.3389/fpls.2013.00266
- Chesus, K. A., & Ocheltree, T. W. (2018). Analyzing root traits to characterize juniper expansion into rangelands. *Journal of Arid Environments*, *150*(December 2017), 1–8. https://doi.org/10.1016/j.jaridenv.2017.12.010
- Chorover, J., Troch, P. A., Rasmussen, C., Brooks, P. D., Pelletier, J. D., Breshears, D. D., ... Durcik, M. (2011). How Water, Carbon, and Energy Drive Critical Zone Evolution: The Jemez–Santa Catalina Critical Zone Observatory. *Vadose Zone Journal*, *10*(3), 884. https://doi.org/10.2136/vzj2010.0132
- Core Team, R. (2015). R: A Language and Environment for Statistical Computing. Vienna, Austria: R Foundation for Statistical Computing. Retrieved from https://www.r-project.org/
- Dore, S., Kolb, T. E., Montes-Helu, M., Eckert, S. E., Sullivan, B. W., Hungate, B. a., ... Finkral, a. (2010). Carbon and water fluxes from ponderosa pine forests disturbed by wildfire and thinning. *Ecological Applications*, 20(3), 663–683. https://doi.org/10.1890/09-0934.1
- Ellison, D., Morris, C. E., Locatelli, B., Sheil, D., Cohen, J., Murdiyarso, D., ... Sullivan, C. A. (2017). Trees, forests and water: Cool insights for a hot world. *Global Environmental Change*, 43, 51–61. https://doi.org/10.1016/j.gloenvcha.2017.01.002
- Falge, E., Baldocchi, D., Olson, R., Anthoni, P., Aubinet, M., Bernhofer, C., ... Wofsy, S. (2001). Gap filling strategies for defensible annual sums of net ecosystem exchange RID A-1625-2009 RID A-7210-2008 RID A-7515-2008 RID G-3882-2010. *Agricultural and Forest Meteorology*, 107(1), 43–69. https://doi.org/10.1016/S0168-1923(00)00225-2
- Garcia-Forner, N., Adams, H. D., Sevanto, S., Collins, A. D., Dickman, L. T., Hudson, P. J., ... Mcdowell, N. G. (2016). Responses of two semiarid conifer tree species to reduced precipitation and warming reveal new perspectives for stomatal regulation. https://doi.org/10.1111/pce.12588
- Gelman, A., & Rubin, D. B. (1992). Inference from iterative simulation using multiple sequences. *Statistical Science*, 7(4), 457–511.
- Gelman, A., Carlin, J. B., Stern, H. S., Dunson, D. B., Vehtari, A., & Rubin, D. B. (2013). Bayesian Data Analysis (3rd ed.). Boca Raton, FL, FL: CRC Press, Taylor & Francis

- Group.
- Gonzalez, P., Garfin, G. M., Breshears, D. D., Brooks, K. M., Brown, H. E., Elias, E. H., ... Udall, B. H. (2018). Southwest. In D. R. Reidmiller, C. W. Avery, D. R. Easterling, K. E. Kunkel, K. L. M. Lewis, T. K. Maycock, & B. C. Stewart (Eds.), *Impacts, Risks, and Adaptation in the United States: Fourth National Climate Assessment, Volume II* (pp. 1101–1184). Washington, D.C.: U.S. Global Change Research Program. https://doi.org/10.7930/NCA4.2018.CH25
- Grantz, K., Rajagopalan, B., Clark, M., & Zagona, E. (2007). Seasonal shifts in the North American monsoon. *Journal of Climate*, 20(9), 1923–1935. https://doi.org/10.1175/JCLI4091.1
- Grossiord, C., Sevanto, S., Borrego, I., Chan, A. M., Collins, A. D., Dickman, L. T., ... McDowell, N. G. (2017). Tree water dynamics in a drying and warming world. *Plant Cell and Environment*, 40(9), 1861–1873. https://doi.org/10.1111/pce.12991
- Grossiord, C., Sevanto, S., Dawson, T. E., Adams, H. D., Collins, A. D., Dickman, L. T., ... McDowell, N. G. (2017). Warming combined with more extreme precipitation regimes modifies the water sources used by trees. *New Phytologist*, *213*(2), 584–596. https://doi.org/10.1111/nph.14192
- Guo, J.S., & Ogle, K. (2018). Antecedent soil water content and vapor pressure deficit interactively control water potential in Larrea tridentata. *New Phytologist*. https://doi.org/10.1111/nph.15374 Key
- Guo, Jessica S., Hungate, B. A., Kolb, T. E., & Koch, G. W. (2018). Water source niche overlap increases with site moisture availability in woody perennials. *Plant Ecology*, 219(6), 719–735. https://doi.org/10.1007/s11258-018-0829-z
- Huang, J., Yu, H., Guan, X., Wang, G., & Guo, R. (2016). Accelerated dryland expansion under climate change. *Nature Climate Change*, *6*(2), 166–171. https://doi.org/10.1038/nclimate2837
- Huang, K., Yi, C., Wu, D., Zhou, T., Zhao, X., Blanford, W. J., ... Li, Z. (2015). Tipping point of a conifer forest ecosystem under severe drought. *Environmental Research Letters*, 10(2), 024011. https://doi.org/10.1088/1748-9326/10/2/024011
- Ibáñez, I., Katz, D. S. W., & Lee, B. R. (2017). The contrasting effects of short-term climate change on the early recruitment of tree species. *Oecologia*, *184*(3), 701–713. https://doi.org/10.1007/s00442-017-3889-1
- IPCC. (2013). Climate Change: The Physical Science Basis. Contribution of Working Group I to the Fifth Assessment Report of the Intergovernmental Panel on Climate Change. In V. B. and P. M. M. Stocker, T.F., D. Qin, G.-K. Plattner, M. Tignor, S.K. Allen, J. Boschung, A. Nauels, Y. Xia (Ed.) (p. 1535). United Kingdom and New York, NY, USA: Cambridge University Press.
- Jia, X., Zha, T., Gong, J., Wang, B., Zhang, Y., Wu, B., ... Peltola, H. (2016). Carbon and water exchange over a temperate semi-arid shrubland during three years of contrasting precipitation and soil moisture patterns. *Agricultural and Forest Meteorology*, 228–229, 120–129. https://doi.org/10.1016/j.agrformet.2016.07.007
- Jones, S. M., & Gutzler, D. S. (2016). Spatial and seasonal variations in aridification across Southwest North America. *Journal of Climate*, *29*(12), 4637–4649. https://doi.org/10.1175/JCLI-D-14-00852.1
- Jung, M., Reichstein, M., Margolis, H. A., Cescatti, A., Richardson, A. D., Arain, M. A., ... Williams, C. (2011). Global patterns of land atmosphere fluxes of carbon dioxide, latent heat, and sensible heat derived from eddy covariance, satellite, and meteorological observations, 116, 1–16. https://doi.org/10.1029/2010JG001566
- Kerhoulas, L. P., Kolb, T. E., & Koch, G. W. (2013). Forest Ecology and Management Tree size, stand density, and the source of water used across seasons by ponderosa pine in

- northern Arizona. *Forest Ecology and Management*, 289, 425–433. https://doi.org/10.1016/j.foreco.2012.10.036
- Kerhoulas, L. P., Kolb, T. E., & Koch, G. W. (2017). The influence of monsoon climate on latewood growth of southwestern ponderosa pine. *Forests*, 8(140). https://doi.org/10.3390/f8050140
- Knowles, J. F., Molotch, N. P., Trujillo, E., & Litvak, M. E. (2018). Snowmelt-Driven Trade-Offs Between Early and Late Season Productivity Negatively Impact Forest Carbon Uptake During Drought. *Geophysical Research Letters*, 45, 3087–3096. https://doi.org/10.1002/2017GL076504
- Kropp, H., Loranty, M., Alexander, H. D., Berner, L. T., Natali, S. M., & Spawn, S. A. (2017). Environmental constraints on transpiration and stomatal conductance in a Siberian Arctic boreal forest. *Journal of Geophysical Research: Biogeosciences*, *122*(3), 487–497. https://doi.org/10.1002/2016JG003709
- Lauenroth, W. K., & Bradford, J. B. (2006). Ecohydrology and the partitioning AET between transpiration and evaporation in a semiarid steppe. *Ecosystems*, *9*(5), 756–767. https://doi.org/10.1007/s10021-006-0063-8
- Law, B. (2005). Carbon dynamics in response to climate and disturbance: Recent progress from multi-scale measurements and modeling in AmeriFlux, 1–9.
- Liu, Y., Schwalm, C. R., Samuels-Crow, K. E., & Ogle, K. (2019). Ecological memory of daily carbon exchange across the globe and its importance in drylands. *Ecology Letters*, 1806–1816. https://doi.org/10.1111/ele.13363
- Loik, M. E., Griffith, A. B., & Alpert, H. (2013). Impacts of long-term snow climate change on a high-elevation cold desert shrubland, California, USA. *Plant Ecology*, *214*(2), 255–266. https://doi.org/10.1007/s11258-012-0164-8
- Mankin, J. S., Smerdon, J. E., Cook, B. I., Williams, A. P., & Seager, R. (2017). The curious case of projected twenty-first-century drying but greening in the American West. *Journal of Climate*, 30(21), 8689–8710. https://doi.org/10.1175/JCLI-D-17-0213.1
- Manrique-Alba, À., Sevanto, S., Adams, H. D., Collins, A. D., Dickman, L. T., Chirino, E., ... McDowell, N. G. (2018). Stem radial growth and water storage responses to heat and drought vary between conifers with differing hydraulic strategies. *Plant Cell and Environment*, 41(8), 1926–1934. https://doi.org/10.1111/pce.13340
- Martínez-Vilalta, J., & Garcia-Forner, N. (2017). Water potential regulation, stomatal behaviour and hydraulic transport under drought: deconstructing the iso/anisohydric concept. *Plant Cell and Environment*, 40(6), 962–976. https://doi.org/10.1111/pce.12846
- Massman, W. J. (2000). A simple method for estimating frequency response corrections for eddy covariance systems. *Agricultural and Forest Meteorology*, *104*(3), 185–198. https://doi.org/10.1016/S0168-1923(00)00164-7
- McDowell, N. G., Williams, A. P., Xu, C., Pockman, W. T., Dickman, L. T., Sevanto, S., ... Koven, C. (2016). Multi-scale predictions of massive conifer mortality due to chronic temperature rise. *Nature Climate Change*, *6*(3), 295–300. https://doi.org/10.1038/nclimate2873
- McDowell, N., Pockman, W. T., Allen, C. D., Breshears, D. D., Cobb, N., Kolb, T., ... Yepez, E. a. (2008). Mechanisms of plant survival and mortality during drought: Why do some plants survive while others succumb to drought? *New Phytologist*, *178*(4), 719–739. https://doi.org/10.1111/j.1469-8137.2008.02436.x
- McDowell, Nate G., Beerling, D. J., Breshears, D. D., Fisher, R. a., Raffa, K. F., & Stitt, M. (2011). The interdependence of mechanisms underlying climate-driven vegetation mortality. *Trends in Ecology and Evolution*, *26*(10), 523–532. https://doi.org/10.1016/j.tree.2011.06.003
- Morillas, L., Pangle, R. E., Maurer, G. E., Pockman, W. T., McDowell, N., Huang, C. W., ...

- Litvak, M. E. (2017). Tree mortality decreases water availability and ecosystem resilience to drought in piñon-juniper woodlands in the southwestern USA. *Journal of Geophysical Research: Biogeosciences*, 3343–3361. https://doi.org/10.1002/2017JG004095
- Mueller, R. C., Scudder, C. M., Porter, M. E., Talbot Trotter, R., Gehring, C. A., & Whitham, T. G. (2005). Differential tree mortality in response to severe drought: Evidence for long-term vegetation shifts. *Journal of Ecology*, *93*(6), 1085–1093. https://doi.org/10.1111/j.1365-2745.2005.01042.x
- Neter, J. (1996). Applied linear statistical models, Volume 1 (4th ed.). Irwin.
- Ogle, K., Barber, J. J., Barron-Gafford, G. a, Bentley, L. P., Young, J. M., Huxman, T. E., ... Tissue, D. T. (2015). Quantifying ecological memory in plant and ecosystem processes. *Ecology Letters*, 221–235. https://doi.org/10.1111/ele.12399
- Parton, W. J. (1978). Abiotic Section of ELM. In G. S. Innis (Ed.), *Grassland Simulation Model. Ecological Studies (Analysis and Synthesis)*, vol. 26. New York, NY.
- Peltier, D. M. P., Fell, M., & Ogle, K. (2016). Legacy effects of drought in the southwestern United States: A multi-species synthesis. *Ecological Monographs*, 86(3), 312–326.
- Peltier, D. M. P., Barber, J., & Ogle, K. (2017). Quantifying antecedent climatic drivers of tree growth in the Southwestern US. *Journal of Ecology*. https://doi.org/10.1111/ijlh.12426
- Petrie, M. D., Pockman, W. T., Pangle, R. E., Limousin, J. M., Plaut, J. A., & Mcdowell, N. G. (2015). Agricultural and Forest Meteorology Winter climate change promotes an altered spring growing season in pine-juniper woodlands pi non. *Agricultural and Forest Meteorology*, 214–215, 357–368. https://doi.org/10.1016/j.agrformet.2015.08.269
- Plummer, M. (2003). JAGS: A program for analysis of Bayesian graphical models using Gibbs sampling. *Proceedings of the 3rd International Workshop on Distributed Statistical Computing (DSC 2003)*, 20–22. https://doi.org/10.1.1.13.3406
- Prein, A. F., Holland, G. J., Rasmussen, R. M., Martyn, P., & Tye, M. R. (2016). Running dry: The U.S. Southwest's drift into a drier climate state. *Geophysical Research Letters*, 43, 1–8. https://doi.org/10.1002/2015GL066727
- Reichstein, M., Falge, E., Baldocchi, D., Papale, D., Aubinet, M., Berbigier, P., ... Valentini, R. (2005). On the separation of net ecosystem exchange into assimilation and ecosystem respiration: Review and improved algorithm. *Global Change Biology*, *11*(9), 1424–1439. https://doi.org/10.1111/j.1365-2486.2005.001002.x
- Reynolds, J. F. (2001). Desertification. In *Encyclopedia of Biodiversity* (pp. 61–78). Academic Press.
- Reynolds, J. F., & Stafford-Smith, D. M. (2002). Do Humans Cause Deserts. In J. F. Reynolds & D. M. Stafford-Smith (Eds.), *Global Desertification: Do Humans Cause Deserts?* (pp. 1–25). Dahlem University Press.
- Ryan, E. M., Ogle, K., Zelikova, T. J., LeCain, D. R., Williams, D. G., Morgan, J. A., & Pendall, E. (2015). Antecedent moisture and temperature conditions modulate the response of ecosystem respiration to elevated CO2 and warming. *Global Change Biology*, *21*(7), 2588–2602. https://doi.org/10.1111/gcb.12910
- Ryan, E. M., Ogle, K., Peltier, D., Walker, A. P., De Kauwe, M. G., Medlyn, B. E., ... Pendall, E. (2017). Gross primary production responses to warming, elevated CO2, and irrigation: quantifying the drivers of ecosystem physiology in a semiarid grassland. *Global Change Biology*, 23(8), 3092–3106. https://doi.org/10.1111/gcb.13602
- Sala, O. E., Lauenroth, W. K., & Parton, W. J. (1992). Long-term soil water dynamics in the shortgrass steppe. *Ecology*, 73(4), 1175–1181.
- Sandvig, R. M., & Phillips, F. M. (2006). Ecohydrological controls on soil moisture fluxes in arid to semiarid vadose zones. *Water Resources Research*, 42(8), 1–20.

- https://doi.org/10.1029/2005WR004644
- Schlaepfer, D. R., Bradford, J. B., Lauenroth, W. K., Munson, S. M., Tietjen, B., Hall, S. A., ... Jamiyansharav, K. (2017). Climate change reduces extent of temperate drylands and intensifies drought in deep soils. *Nature Communications*, 8, 1–9. https://doi.org/10.1038/ncomms14196
- Schwalm, C. R., Williams, C. a., Schaefer, K., Baldocchi, D., Black, T. A., Goldstein, A. H., ... Scott, R. L. (2012). Reduction in carbon uptake during turn of the century drought in western North America. *Nature Geoscience*, *5*(8), 551–556. https://doi.org/10.1038/ngeo1529
- Seager, R., Ting, M., Held, I., Kushnir, Y., Lu, J., Vecchi, G., ... Naik, N. (2007). Model projections of an imminent transition to a more arid climate in southwestern North America. *Science (New York, N.Y.)*, *316*(5828), 1181–1184. https://doi.org/10.1126/science.1139601
- Seager, R., & Ting, M. (2017). Decadal Drought Variability Over North America:

  Mechanisms and Predictability. *Current Climate Change Reports*, *3*(2), 141–149. https://doi.org/10.1007/s40641-017-0062-1
- Shaw, J. D., Steed, B. E., & Deblander, L. T. (2005). Forest Inventory and Analysis (FIA) Annual Inventory Answers the Question: What Is Happening to Pinyon-Juniper Woodlands? *Journal of Forestry*, 103(6), 280–285.
- Spiegelhalter, D. J., Best, N. G., Carlin, B. P., & van der Linde, A. (2002). Bayesian Measures of Model Complexity and Fit. *Journal of the Royal Statistical Society Series B* (Statistical Methodology), 64(4), 583–639. https://doi.org/10.1111/1467-9868.00353
- Spiegelhalter, D. J., Best, N. G., Carlin, B. P., & van der Linde, A. (2014). The deviance information criterion: 12 years on. *Journal of the Royal Statistical Society: Series B* (Statistical Methodology), 76(3), 485–493. https://doi.org/10.1111/rssb.12062
- Szejner, P., Wright, W. E., Babst, F., Belmecheri, S., Trouet, V., Leavitt, S. W., ... Monson, R. K. (2016). Latitudinal gradients in tree ring stable carbon and oxygen isotopes reveal differential climate influences of the North American Monsoon System. https://doi.org/10.1002/2016JG003460.Received
- Ting, M., Seager, R., Li, C., Liu, H., & Henderson, N. (2018). Mechanism of future spring drying in the Southwestern United States in CMIP5 models. *Journal of Climate*, *31*(11), 4265–4279. https://doi.org/10.1175/JCLI-D-17-0574.1
- Trenberth, K. E., Dai, A., Van Der Schrier, G., Jones, P. D., Barichivich, J., Briffa, K. R., & Sheffield, J. (2014). Global warming and changes in drought. *Nature Climate Change*, 4(1), 17–22. https://doi.org/10.1038/nclimate2067
- Vargas, R., Detto, M., Baldocchi, D. D., & Allen, M. F. (2010). Multiscale analysis of temporal variability of soil CO 2 production as influenced by weather and vegetation. *Global Change Biology*, *16*(5), 1589–1605. https://doi.org/10.1111/j.1365-2486.2009.02111.x
- Vivoni, E. R., Moreno, H.A., Mascaro, G., Rodriguez, J. C., Watts, C. J., Garatuza-Payan, J., & Scott, R. L. (2008). Observed relation between evapotranspiration and soil moisture in the North American monsoon region. *Geophysical Research Letters*, *35*(22), 1–6. https://doi.org/10.1029/2008GL036001
- Voelker, S. L., DeRose, R. J., Bekker, M. F., Sriladda, C., Leksungnoen, N., & Kjelgren, R. K. (2018). Anisohydric water use behavior links growing season evaporative demand to ring-width increment in conifers from summer-dry environments. *Trees Structure and Function*, 32(3), 735–749. https://doi.org/10.1007/s00468-018-1668-1
- Wang, K., & Dickinson, R. E. (2012). A review of global terrestrial evapotranspiration: observation, modelling, climatology, and climatic variability. *Review of Geophysics*, 50(2011), 1–54. https://doi.org/10.1029/2011RG000373.1.INTRODUCTION

- Webb, E., Pearman, G., & Leuning, R. (1980). Correction of flux measurements for density effects due to heat and water vapour transfer. *Quarterly Journal of The*, 106, 85–100. Retrieved from http://www3.interscience.wiley.com/journal/114056302/abstract
- West, A. G., Hultine, K. R., Burtch, K. G., & Ehleringer, J. R. (2007). Seasonal variations in moisture use in a pinon juniper woodland. *Oecologia*, 153, 787–798. https://doi.org/10.1007/s00442-007-0777-0
- Williams, A. P., Allen, C. D., Macalady, A. K., Griffin, D., Woodhouse, C. a., Meko, D. M., ... McDowell, N. G. (2012). Temperature as a potent driver of regional forest drought stress and tree mortality. *Nature Climate Change*, *3*(3), 292–297. https://doi.org/10.1038/nclimate1693
- Williams, C. A., Hanan, N., Scholes, R. J., & Kutsch, W. (2009). Complexity in water and carbon dioxide fluxes following rain pulses in an African savanna. *Oecologia*, *161*(3), 469–480. https://doi.org/10.1007/s00442-009-1405-y
- Xia, J., Ning, L., Wang, Q., Chen, J., Wan, L., & Hong, S. (2016). Vulnerability of and risk to water resources in arid and semi-arid regions of West China under a scenario of climate change. *Climatic Change*, 549–563. https://doi.org/10.1007/s10584-016-1709-y
- Zhang, K., Kimball, J. S., Nemani, R. R., Running, S. W., Hong, Y., Gourley, J. J., & Yu, Z. (2015). Vegetation Greening and Climate Change Promote Multidecadal Rises of Global Land Evapotranspiration. *Scientific Reports*, 5(June), 1–9. https://doi.org/10.1038/srep15956
- Zhang, Y., Chiew, F. H. S., Jorge, P.-A., Sun, F., Li, H., & Leuning, R. (2017). Global variation of transpiration and soil evaporation and the role of their major climate drivers. *Journal of Geophysical Research: Atmospheres*, 5138–5158. https://doi.org/10.1002/2015JD024584.Received
- Zhang, Y., Peña-Arancibia, J. L., McVicar, T. R., Chiew, F. H. S., Vaze, J., Liu, C., ... Pan, M. (2016). Multi-decadal trends in global terrestrial evapotranspiration and its components. *Scientific Reports*, 6(January), 1–12. https://doi.org/10.1038/srep19124
- Zomer, R. J., Bossio, D. A., Trabucco, A., Yuanjie, L., Gupta, D. C., & Singh, V. P. (2007). Trees and Water: Smallholder Agroforestry on Irrigated Lands in Northern India. Colombo, Sri Lanka.
- Zomer, R. J., Trabucco, A., Bossio, D. A., & Verchot, L. V. (2008). Climate change mitigation: A spatial analysis of global land suitability for clean development mechanism afforestation and reforestation. *Agriculture, Ecosystems and Environment*, 126(1–2), 67–80. https://doi.org/10.1016/j.agee.2008.01.014

Acce

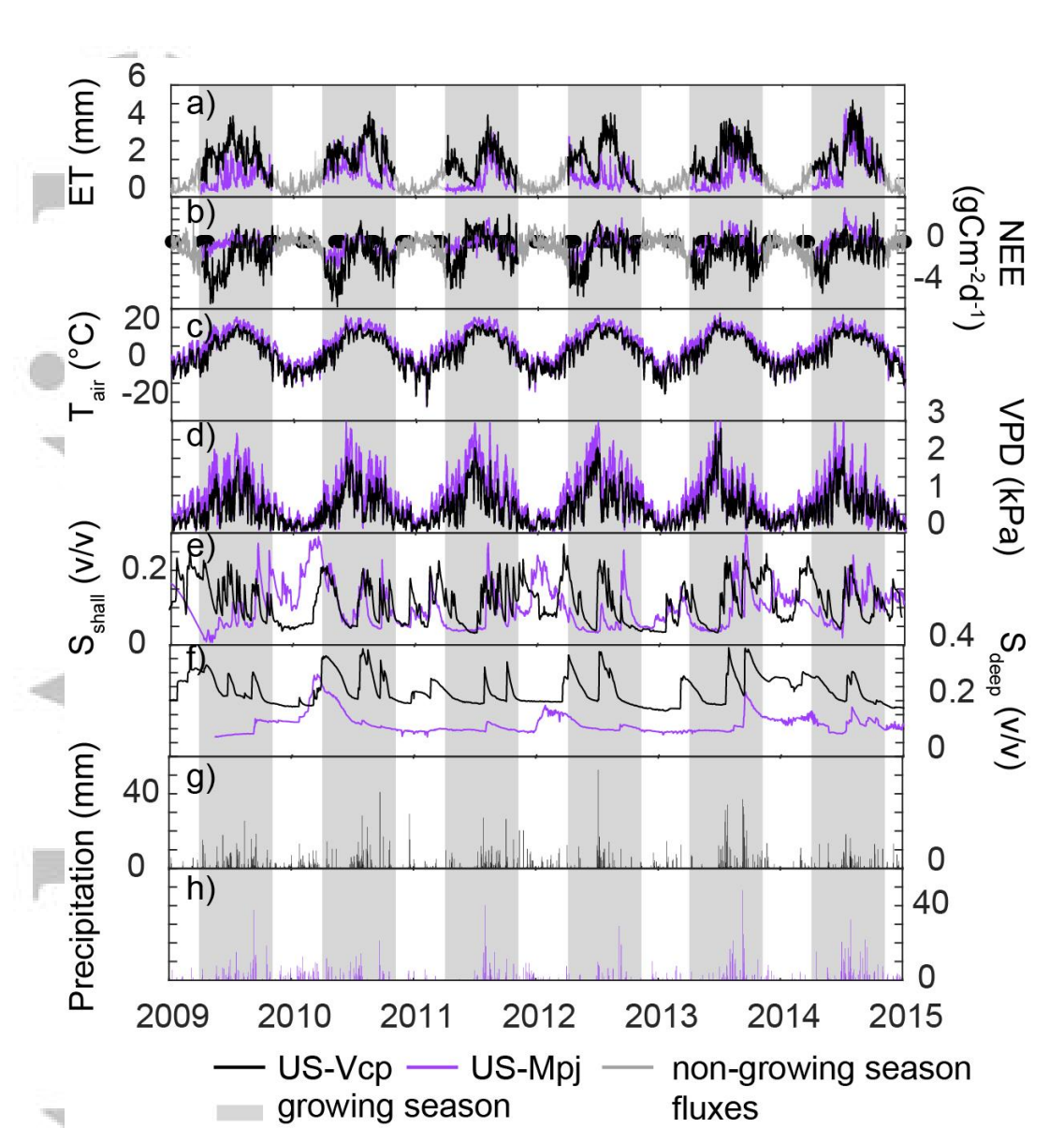


Figure 1. Observed time-series of daily (a) evapotranspiration (ET), (b) net ecosystem exchange (NEE) of  $CO_2$ , (c) air temperature ( $T_{air}$ ), (d) vapor pressure deficit (VPD), (e) shallow soil water content (0-5 cm,  $S_{shall}$ ), (f) deep soil water content (25-30 cm,  $S_{deep}$ ), (g) precipitation at US-Vcp, and (h) precipitation at US-Mpj. Purple lines at the pinyon-juniper site (US-Mpj) and black lines at the ponderosa pine site (US-Vcp) represent the modeled growing season fluxes (panels a and b) and the full covariate datasets. Gray lines in panels a and b represent non-growing season fluxes that were not included as response variables in the models. Vertical gray shaded regions denote the growing season period, corresponding to the time periods represented in Figures 4 and 5.

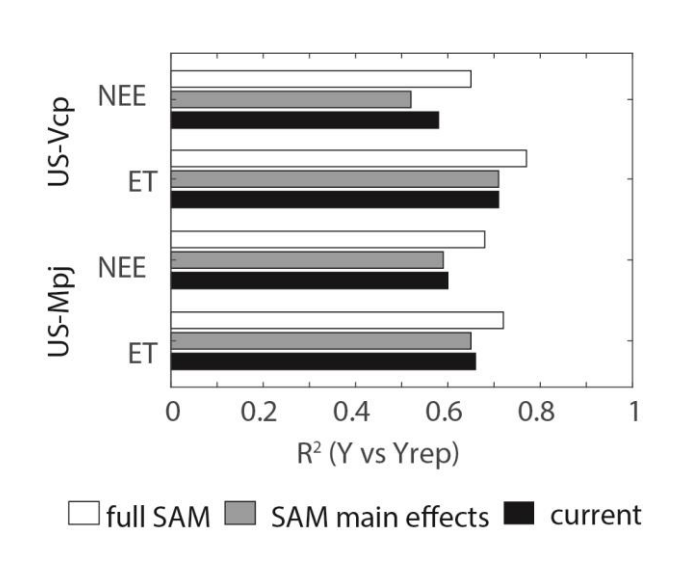


Figure 2. Comparison of model fit (coefficient of determination, R<sup>2</sup>) between measured (Y) and modeled (Yrep) ET and NEE fluxes, for models that consider current covariates only (black bars), main effects only in the SAM framework (gray bars), and the full SAM model with main effects, quadratic terms, and interactive effects (white bars). Groups of bars are shown for each site (ponderosa pine = US-Vcp and pinyon-juniper = US-Mpj) and variable (NEE or ET) combination.

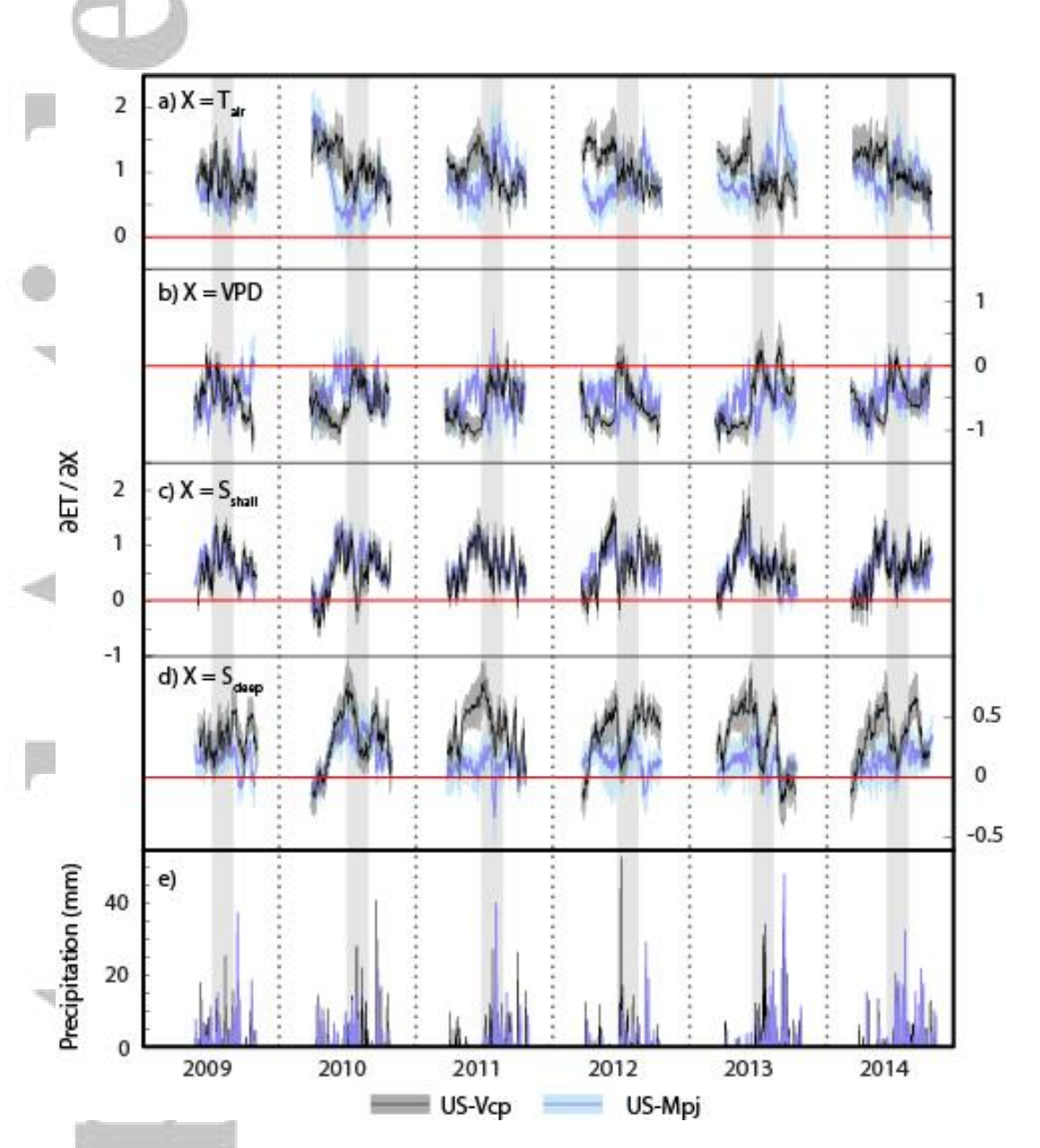


Figure 3. Variation in the net sensitivity of ET to environmental drivers (X),  $\partial ET/\partial X$ , for: (a) air temperature ( $T_{air}$ ), (b) vapor pressure deficit (VPD), (c) shallow soil water content ( $S_{shall}$ ), and (d) deep soil water content ( $S_{deep}$ ), within growing seasons and across years at US-Mpj (purple lines) and US-Vcp (gray lines), along with (e) observed daily precipitation. The solid purple and black lines are the posterior means for  $\partial ET/\partial X$ , and the shaded blue and gray regions are the corresponding 95% credible intervals (CIs). The horizontal red lines indicate  $\partial ET/\partial X=0$ ; the dotted vertical lines separate years; the gray vertical bars indicate the average timing of the North American Monsoon onset (early July) and retreat (early September) in New Mexico.



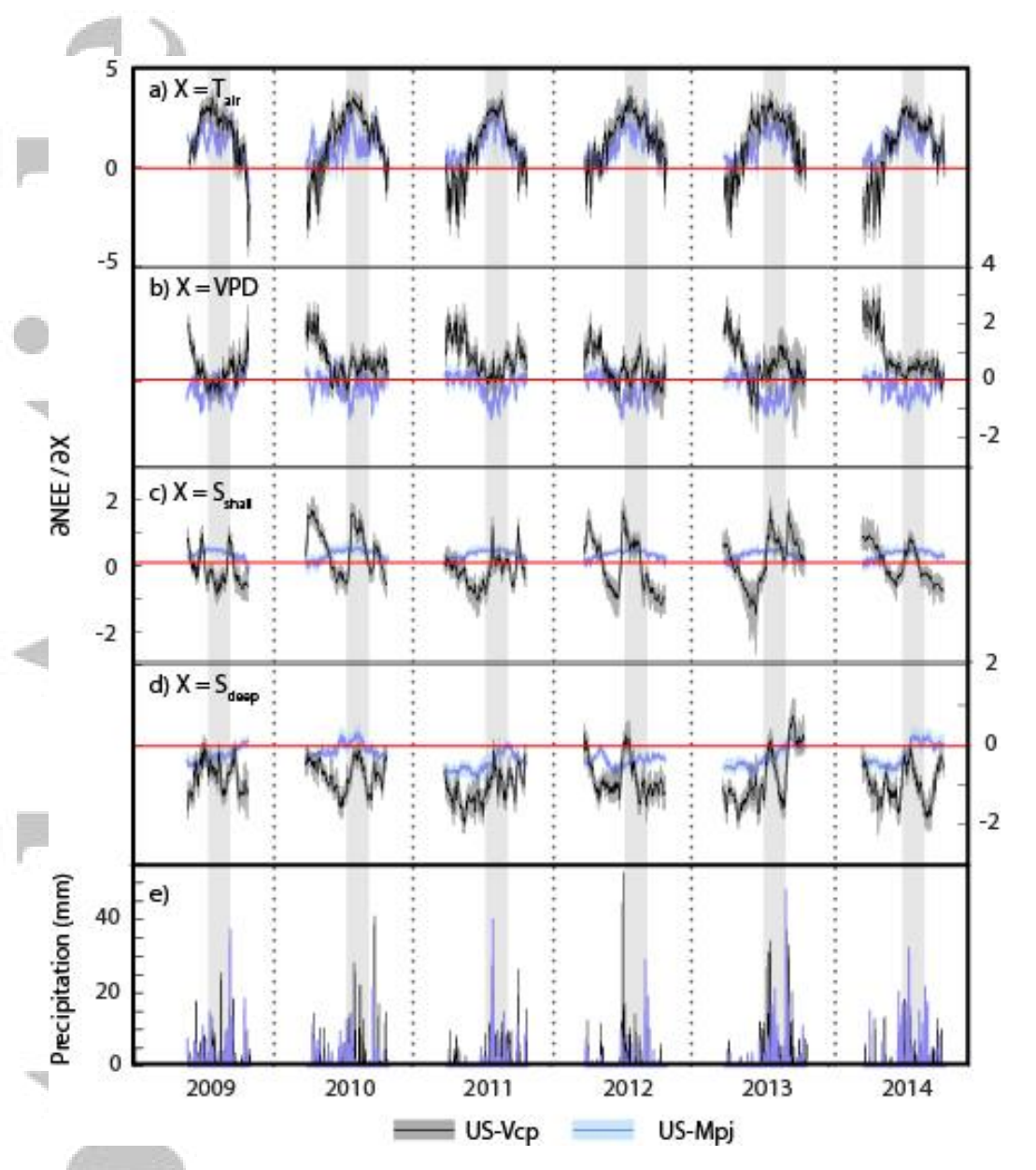


Figure 4. Variation in the net sensitivity of NEE to (a)  $T_{air}$ , (b) VPD, (c)  $S_{shall}$ , and (d)  $S_{deep}$  within growing seasons and across years at US-Mpj (purple) and US-Vcp (gray), along with (e) observed daily precipitation. See Fig. 4 for more details.



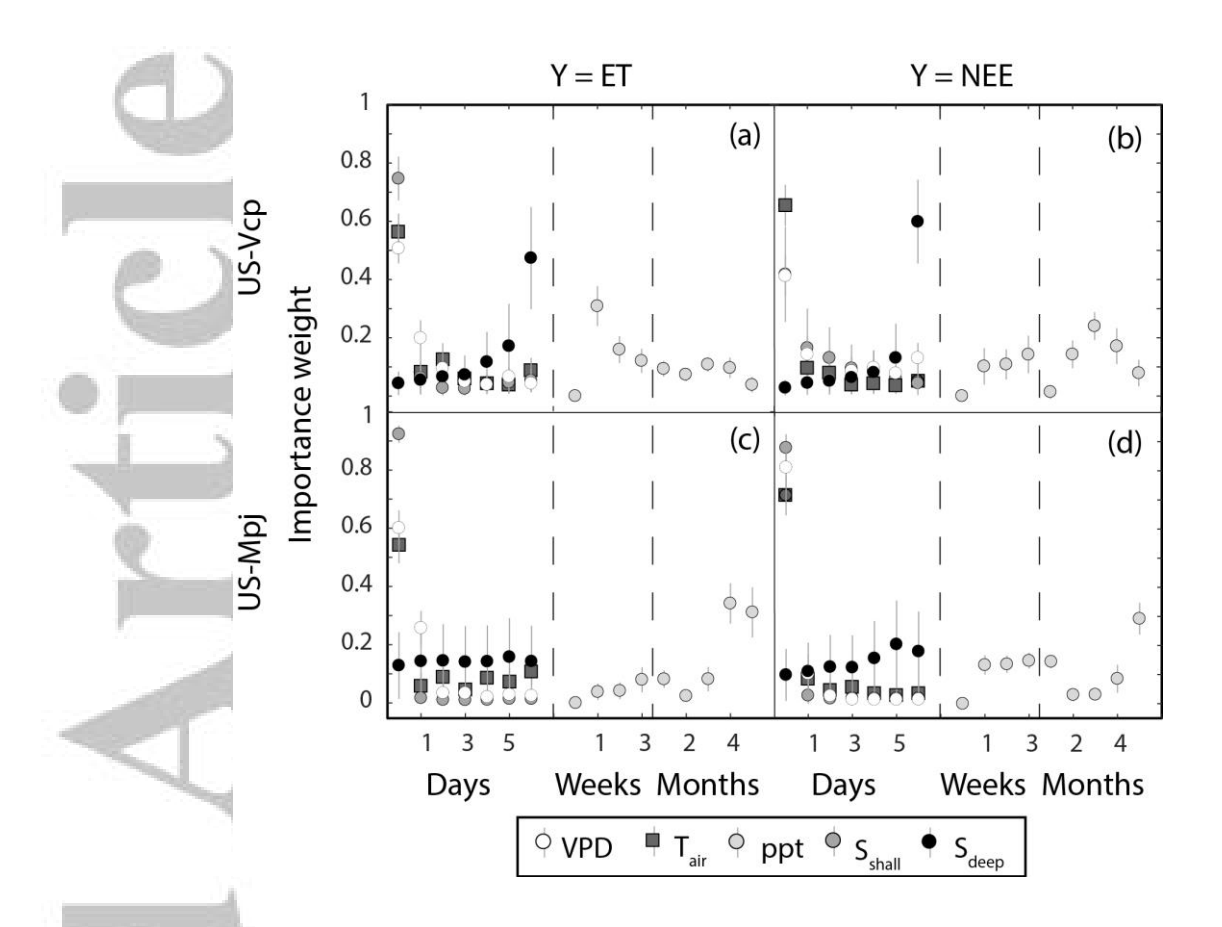


Figure 5. Posterior means and 95% credible intervals (CIs) for the antecedent importance weights ( $w_{j,t}$ , equation 2) for driving variables of (a) ET at US-Vcp, (b) NEE at US-Vcp, (c) ET at US-Mpj, and (d) NEE at US-Mpj. Symbols are colored according to the driving variable, with the atmospheric variables being VPD and  $T_{air}$ , and the moisture-related variables being precipitation (ppt),  $S_{shall}$ , and  $S_{deep}$  (see Fig. 1 for definitions of these variables). The vertical dashed lines denote a change in the temporal scale.

Table 1. Summary of posterior estimates of the effects parameters in the full SAM model (see equation 1), for each response variable (Y) and site combination. Within each cells, the direction of the effect (+/-) is indicated, and cells are shaded by Bayesian p-values, with darker shading denoting greater significance\*. See Tables S1a and S1b in the supplemental materials for numerical estimates (i.e., posterior means and 95% credible intervals). See Fig. 1 for definitions of the covariates and site names.

9		Y = ET		Y = NEE	
Effect parameter	Covariate	US-Vcp	US-Mpj	US-Vcp	US-Mpj
$\beta_1$	$T_{air}$	+	+	n.s	+
$eta_2$	VPD	-	-	+	+
$\beta_3$	$S_{shall}$	+	+	+	+
$eta_4$	$S_{deep}$	+	+	-	-
$eta_5$	precipitation	-	+	n.s	n.s
$oldsymbol{eta}_6$	PAR	+	+	-	-
$\beta_7$	$\Delta \mathrm{VPD}$	+	n.s	-	n.s
$oldsymbol{eta}_8$	$\mathrm{VPD}^2$	n.s	+	n.s	+
$oldsymbol{eta}_{9}$	Tair <sup>2</sup>	n.s	n.s	+	+
$eta_{1,2}$	$T_{air} \times VPD$	+	n.s	-	-
$\beta_{1,3}$	$T_{air} \times S_{shall}$	n.s	+	n.s	+
$\beta_{1,4}$	$T_{air} \times S_{deep}$	+	+	n.s	+
$eta_{1,5}$	$T_{air} \times precipitation$	-	-	n.s	-
$\beta_{2,3}$	$VPD \times S_{shall}$	+	+	+	n.s
$eta_{2,4}$	$VPD \times S_{\text{deep}}$	-	-	+	-
$eta_{2,5}$	VPD × precipitation	+	+	-	+
$eta_{3,4}$	$S_{shall} \times S_{deep}$	-	-	+	n.s
$eta_{3,5}$	$S_{shall} \times precipitation$	+	+	-	n.s
$\beta_{4,5}$	$S_{deep} \times precipitation$	-	+	+	+

<sup>\*</sup>Definitions of shading as defined by Bayesian p-values: